Gamma-gamma absorption in gamma-ray binary systems

DC du Plooy, B van Soelen

Department of Physics, University of the Free State, Bloemfontein, South Africa

Abstract:

Gamma-ray binaries are a class of high-mass binary systems which are distinguished by their spectral energy distributions peaking above 1 MeV. Gamma-ray binaries consist of an O or B type companion and an orbiting compact object which is either a neutron star or a black hole. Generally in these systems the nature of the compact object is unknown except for two cases, namely PSR B1259-63 and PSR J2032+4127, where the compact objects have been identified to be pulsars. For a neutron star compact object the non-thermal emission is believed to originate from the interaction between the stellar and pulsar winds. It has been suggested that there are multiple regions of emission in these systems with the GeV and TeV emission potentially originating from different locations. The influence of gamma-gamma absorption on the gamma-ray emission may, therefore, be a tool in constraining the location of the TeV emission region. We have calculated the gamma-gamma absorption expected around six of the seven known gamma-ray binaries and are studying the influence on the observed spectrum. With this we plan to place constraints on the TeV production location. The results of this study will be used for predictions based on the upcoming Cherenkov Telescope Array (CTA).

Introduction:

The nature of the compact object in γ-ray binaries is only known in two of the nine systems discovered so far, namely PSR B1259-63/LS 2883 and PSR J2032+4127, which both harbour a pulsar, identified by pulsed radio or γ-ray emission (Johnston et al. 1992, Camilo et al. 2009). Gamma-ray binaries produce unpulsed, non-thermal radiation from radio up to TeV energy γ-rays. The TeV emission is produced via inverse Compton scattering of electrons off stellar photons. If the compact object in all systems is a neutron star, it is believed to have sufficient rotational velocity to halt accretion from the companion stellar wind. Due to the stellar winds having a higher ram pressure than the pulsar winds, this leads to the formation of a cometary tail double shock around the pulsar, consisting of shocked pulsar and stellar wind material. It is often assumed that the TeV emission originates from particle acceleration close to the apex of the shock, situated between the companion star and pulsar, but the shocked material further down the tail may provide an alternative particle acceleration region. At this region, called the Coriolis turnover, a secondary shock could occur which might lead to additional TeV emission, as demonstrated by numerical simulations by Bosch-Ramon et al. (2012). The possibility of a black hole compact object cannot be ruled out and has been the subject of debate for many systems, most notably for LS I+61°303. In the past, radio observations have shown signs of possible jet-like structures from LS I+61°303 (Massi and Torricelli-Ciamponi, 2014; Massi et al. 1993, 2002, 2004, Taylor et al., 2000) and, furthermore, is the only system to show a consistent superorbital period of 1667±8 days which could be explained by a precessing jet model (Jaron et al. 2016; Massi and Torricelli-Ciamponi, 2014, 2016). In this scenario, the system would be a microquasar where the γ-rays are produced via Compton scattering close to the base of the relativistic jet (Yamaguchi et al. 2010).

Theory:

The geometry of the γ-ray attenuation in the binary system is shown in Fig. 1. A γ-ray, with energy E_γ, travelling in the direction $\overrightarrow{e_\gamma}$ and a stellar photon, with energy $\epsilon_\star$, travelling in the direction $\overrightarrow{e_\star}$, will interact and undergo γγ absorption at P. The optical depth due to γγ absorption can be determined by applying a quadruple integral over the path length l, the solid angle $d\Omega = \sin d\theta \; d\theta d\phi$, and the energy of stellar photon ϵ

$$\tau_{\gamma\gamma} = \int_{\ell_{\max}}^{\ell_{\min}} \int_{\mu_{\min}}^{1} \int_{0}^{2\pi} \int_{\epsilon_{\min}}^{\epsilon_{\max}} n_\epsilon \sigma_{\gamma\gamma} \left(1 - \overrightarrow{e_\gamma} \cdot \overrightarrow{e_\star}\right) d\epsilon \, d\phi \, d\mu \, dl \,,$$

where $\mu = \cos\theta$, $\mu_{\min} = \left(1 - \frac{R_\star^2}{d^2}\right)^{1/2}$, d is the distance to the centre of the star from P, and n_ϵ is the stellar photon density. The γγ-cross section $\sigma_{\gamma\gamma}$ is given by

$$\sigma_{\gamma\gamma} = \frac{3}{16} \sigma_T (1-\beta^2) \left[(3-\beta^4) \, ln\left(\frac{1+\beta}{1-\beta}\right) - 2\beta(2-\beta^2)\right],$$

where σ_T is the Thomson cross section and

$$\beta^2 = 1 - \frac{2 m_e c^4}{\epsilon E_\gamma \left(1 - \overrightarrow{e_\gamma} \cdot \overrightarrow{e_\star}\right)},$$

where m_e is the electron mass, c is the speed of light, and the term $\left(1 - \overrightarrow{e_\gamma} \cdot \overrightarrow{e_\star}\right)$ describes the angular dependency of the opacity (Dubus, 2006).

The distance to the apex of the shock, or the "stand-off distance", can be determined from the ratio of the stellar ($p_{\rm sw}$) and pulsar ($p_{\rm pw}$) ram pressures

$$\mathrm{R_s} = D \times \frac{\sqrt{\eta}}{1+\sqrt{\eta}} \,,$$

where $\eta \; is$

$$\eta = \frac{p_{\rm sw}}{p_{\rm pw}} \,.$$

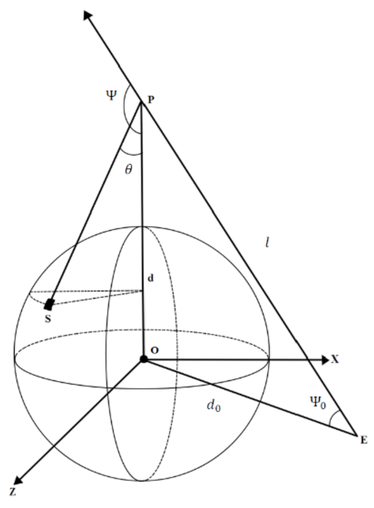

Figure 1. The geometry of γγ absorption which occurs at position P due to $e^- e^+$ pair production between a stellar photon emitted from the surface of the star at position S and a γ-ray photon emitted at position E. The γ-ray is emitted at an angle Ψ_0 (Dubus 2006), relative to the stellar centre (along the line PE), and travels a distance l towards an interaction point P.

Results:

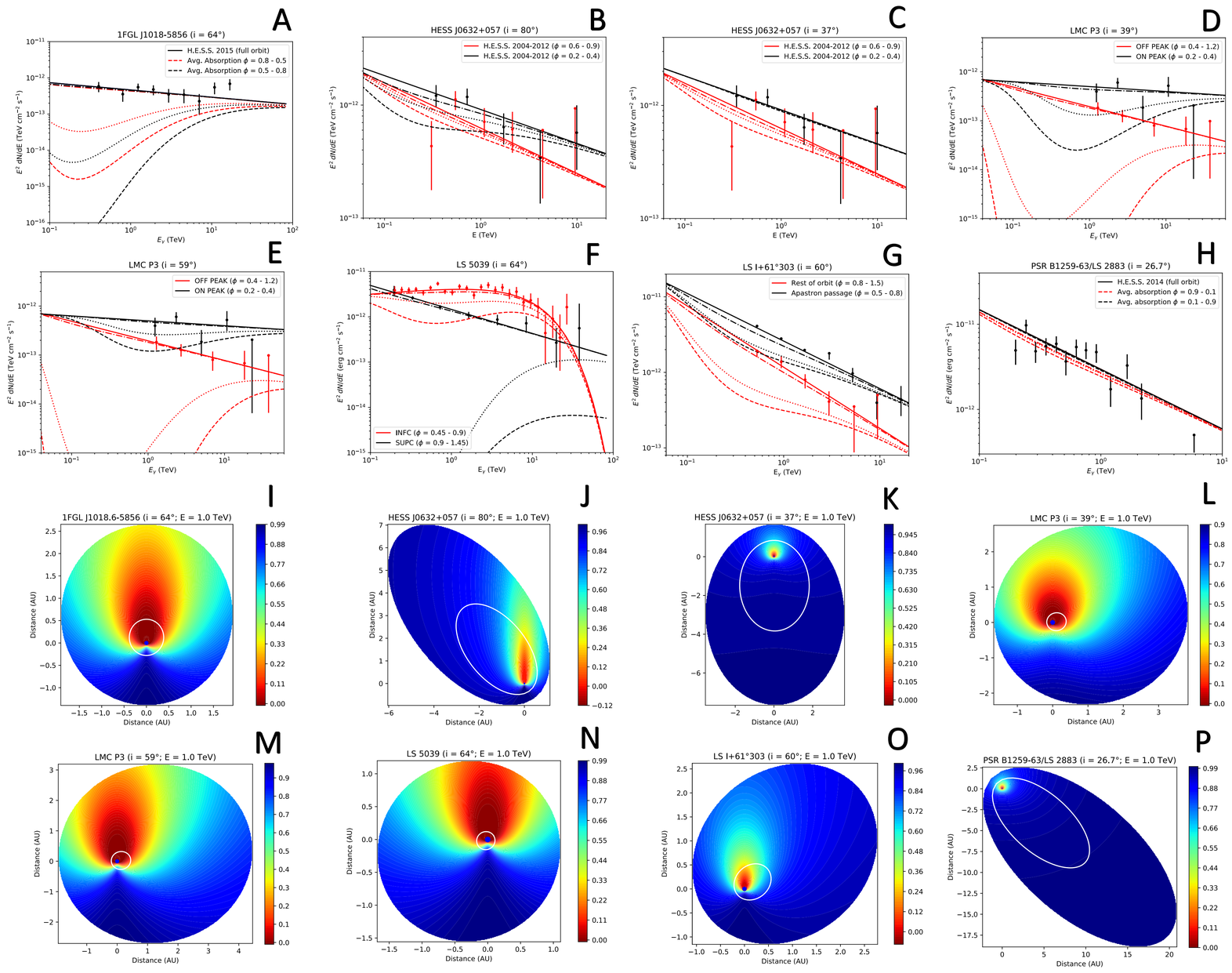

Figure 1: **A – H**: Spectral energy distributions (SED) of all γ-ray binaries for specific orbital phases as indicated in the legend on each plot. The parameters used are given in Table. 1. Each SED includes three absorption curves corresponding to the stand-off distance (dashed), the binary separation (dotted), and the distance of negligible absorption (dashdot), which is taken as when $\exp(-\tau_{\gamma\gamma}) \geq 0.94$. The distance at which absorption becomes negligible ($D_{\rm neg,h}$) and ($D_{\rm neg,s}$) is given in Table 1 in units of the binary separation (D) and corresponds to the harder and softer spectrum respectively.

I - P: Absorption maps using the same parameters as used for the SEDs. The colour gradient indicates the level of attenuation as $\exp(-\tau_{\gamma\gamma})$. The optical star is indicated by a blue circle at the origin and the white ellipse shows the orbit of the compact object. For all plots, the observer is viewing the binary system from the bottom of the page.

Parameters:

The results presented were modelled using the parameters given in Table. 1. All of the parameters are for a neutron star compact object.

	LS 5039[†]	PSR B1259-63[▲]	1 FGL J2018.6-5856[•]	LS I 61° 303[▼]	HESS J0632+057[■]	LMC P3[‡]
P_{orb} (days)	3.90603	1236.724526	16.544	26.496	315	10.301
e	0.24	0.86987970	0.31	0.54	0.83	0.40
ω(°)	212	138.665013	89	41	129	11
i (°)	64	26.7	64	60	37 & 80	39 & 59
$M_\star$ ($M_\odot$)	23	29.8	31	12	16	25 & 42
M_{comp} ($M_\odot$)	1.4	1.4	1.4	1.4	1.4	1.4
$R_\star$ ($R_\odot$)	9.3	9.2	10.1	10	8	15
$T_\star$ (K)	39000	33500	38900	22500	30000	40000
η	0.1	0.07	0.01	0.3	1.0	0.05
z	0.76	0.79	0.91	0.65	0.5	0.82
$D_{\rm neg,h}$	10	2	20	2	2	10 & 10
$D_{\rm neg,s}$	70	2	30	4	2	50 & 50

▲ Shannon et al. (2014); Miller-Jones et al. (2018); Negueruela at al. (2011), Chen et al. (2019)
● An et al. (2015); Monageng et al. (2017); Napoli et al. (2011)
▼ McSwain et al. (2004); Aragona et al. (2009), Sierpowska-Bartosik et al. (2009)
■ Casares et al. (2012); Aliu et al. (2014); Aragona et al. (2010), Archer et al. (2020)
al. (2012); McSwain et al. (‡ Corbet et al. (2016); Pietrzyn´ski, et al. (2013); van Soelen, et al. 2019

Discussion and Conclusion:

Due to the high angular dependency of inverse Compton scattering the maximum GeV and TeV emission should, to a first approximation, occur at superior conjunction. However, superior conjunction is also the phase which is most favourable for $\gamma\gamma$ absorption and this will lead to a high attenuation of TeV photons. The maximum TeV emission may then instead occur around inferior conjunction where the effects of γγ absorption is significantly less (Dubus 2006a, 2006b). Since the effect of γγ absorption is known to be important, in this work we have undertaken a detailed study of the level of attenuation for known γ-ray binaries that can be observed with CTA and that have known binary solutions. From these figures it is apparent that regions around superior conjunction shows significant absorption. In Fig. 1 (A – H) we show the results of $\gamma\gamma$ absorption for various distances and averaged over the same phases as the reported TeV observations. If the observed TeV emission originates from the apex of the shock it must be affected by γγ absorption. This should result in a low energy cut-off around $\sim$ 1 TeV. However, observations do not clearly show this effect. This suggests that either the contribution from cascade emission must be significant, or that emission must occur further out along the shock as suggested by e.g. Zabalza et al. (2013). The main objective of these results is to make predictions on possible locations of the TeV emission which can be tested with the upcoming Cherenkov Telescope Array. The improved sensitivity of the CTA instruments (Actis et al. 2011) will be able to detect smaller variations in emission such as curvature which could be reconciled with the $\gamma\gamma$ absorption curves. Furthermore, the effects of $\gamma\gamma$ is more significant to energies $\sim$ 100 GeV and decreases for energies $>$ 1 TeV, which may lead to a hardening of the spectrum when the absorption is higher. This may be detectable with CTA.

References:

Actis, M., Agnetta, G., Aharonian, F., et al. 2011, ExA, 32, 193
Aliu, E., Archambault, S., Aune, T., et al. 2014, ApJ, 780, 168
An, H., Bellm, E., Bhalerao, V., et al. 2015, ApJ, 806, 166
Aragona, C., McSwain, M. V., Grundstrom, E. D., et al. 2009, ApJ, 698, 514
Aragona, C., McSwain, M. V., & De Becker, M. 2010, ApJ, 724, 306
Archer, A., Benbow, W., et al. 2020, ApJ, 888, 115
Bosch-Ramon, V., Barkov, M. V., Khangulyan,D., & Perucho, M. 2012, A&A, 544, A59
Böttcher, M. & Dermer, C. D. 2005, ApJ, 634, L81
Camilo, F., Ray, P. S., Ransom, S. M., Burgay, M., Johnson, T. J., Kerr, M., Gotthelf, E. V., et al. 2009, ApJ, 705, 1
Casares, J., Ribó, M., Ribas, I., et al. 2012, MNRAS, 421, 1103
Chen, A. M., Takata, J., Yi, S. X., Yu, Y. W., et al. 2013, A&A, 627, 87
Corbet, R. H. D., Chomiuk, L., Coe, M. J., et al. 2016, ApJ, 829, 105
Dubus, G. 2006a, A&A, 451, 9
Dubus, G. 2006b, A&A, 456, 3
Fermi/LAT collaboration, Ackermann, M. & Ajello, M., et al. 2012, Science, 335, 189
Gould, R. J. & Schréder, G. P. 1967, Physics Review, 155, 1404
H.E.S.S. Collaboration et al. 2018, A&A, 610, L81
Jauch, J. M. & Rohrlich, F. 1967, Texts and Monographs in Physics 2nd ed. (New York: Springer)
Jaron, F., Torricelli-Ciamponi, G., & Massi, M. 2016, A&A, 595, A92
Massi, M., & Torricelli-Ciamponi, G., 2014, A&A, 564, 23
Massi, M., & Torricelli-Ciamponi, G., 2016, A&A, 585, 123
Massi, M., Paredes, J. M., et al. 1993, A&A, 269, 249
Massi, M., Ribó, M., et al. 2002, Proceedings of the 6th EVN Symposium, 279
Massi, M., Ribó, M., et al. 2004, A&A, 414, 1
McSwain, M. V., Gies, D. R., Huang, W., et al. 2004, ApJ, 600, 927
Miller-Jones, J. C. A., Deller, A. T., Shannon, R. M., et al. 2018, MNRAS, 479, 4849
Monageng, I. M., McBride, V. A., Townsend, L. J., et al. 2017, ApJ, 847, 68
Napoli, V. J., McSwain, M. V., Marsh Boyer, A. N., & Roettenbacher, R. M. 2011, PASP, 123, 1262
Negueruela, I., Ribó, M., Herrero, A., et al. 2011, ApJ, 732, L11
Pietrzyn´ski, G., Graczyk, D., Gieren, W., et al. 2013, Nature, 495, 76
Ribó, M., Paredes, J. M., Romero, G. E., et al. 2002, A&A, 384, 954
Sarty, G. E., Szalai, T., Kiss, L. L., et al. 2011, MNRAS, 411, 1293
Shannon, R. M., Johnston, S., & Manchester, R. N. 2014, MNRAS, 437, 3255
Sierpowska-Bartosik, A. & Torres, D. F. 2009, ApJ, 693, 1462
Taylor, A. R., Dougherty, S. M., Scott, W. K., Peracaula, M., & Paredes, J. M. 2000, Astrophysical Phenomena Revealed by Space VLBI, 223
van Soelen, B., Komin, N., Kniazev, A., Väisänen, P. 2019, MNRAS, 484, 4347V
van Soelen, B., & Sushch, I., 2017, ApJ, 837, 175
Yamaguchi, M. S., & Takahara, F. 2010, ApJ, 717, 85Y
ZabalzaV., Bosch-Ramon V., et al. 2013. A&A 551, A17

duplooydc@ufs.ac.za | **www.ufs.ac.za**

UFSUV | UFSweb | UFSweb

The 9th International Fermi Symposium (FERMI2021)

Online conference 12th - 17th April, 2021